

THE DISCOVERY OF AN EVOLVING DUST SCATTERED X-RAY HALO AROUND GRB 031203

S. VAUGHAN¹, R. WILLINGALE¹, P. T. O'BRIEN¹, J. P. OSBORNE¹, J. N. REEVES^{2,3}, A. J. LEVAN¹, M. G. WATSON¹, J. A. TEDDS¹, D. WATSON⁴, M. SANTOS-LLEÓ⁵, P. M. RODRÍGUEZ-PASCUAL⁵, N. SCHARTEL⁵

Draft version December 4, 2018

ABSTRACT

We report the first detection of a time-dependent, dust-scattered X-ray halo around a gamma-ray burst. GRB 031203 was observed by *XMM-Newton* starting six hours after the burst. The halo appeared as concentric ring-like structures centered on the GRB location. The radii of these structures increased with time as $t^{1/2}$, consistent with small-angle X-ray scattering caused by a large column of dust along the line of sight to a cosmologically distant GRB. The rings are due to dust concentrated in two distinct slabs in the Galaxy located at distances of 880 and 1390 pc, consistent with known Galactic features. The halo brightness implies an initial soft X-ray pulse consistent with the observed GRB.

Subject headings: gamma rays: bursts — X-rays: general — Galaxy: structure — ISM:dust

1. INTRODUCTION

It has long been realized that the small-angle scattering of X-rays by dust grains can result in a detectable X-ray “halo” around a distant X-ray source (Overbeck 1965), with a radial intensity distribution that depends on the dust properties and location. This phenomenon was first detected by Rolf (1983) using data from *Einstei*n and confirmed by later observations (e.g. Mauche & Gorenstein 1986; Predehl et al. 1991).

In the case of Gamma-Ray Bursts (GRBs), the transient nature of the burst combined with the large initial X-ray flux means X-ray scattering may be visible for a short period of time with a relatively high surface brightness. As the transient flux passes through a dust slab between the observer and the GRB, the scattering process introduces a time-delay in which the X-rays at larger angles to the line of sight arrive increasingly delayed with respect to the non-scattered X-rays. Thus, the dust allows us to view the GRB X-ray flux at earlier times. The time-dependent X-ray halo around the GRB can, in principle, be used to provide detailed information on the location, spatial distribution and properties of the dust and the distance to and brightness of the GRB (e.g. Trümper & Schöfeler 1973; Klose 1994; Miralda-Escudé 1999; Draine 2003). Images of transient X-ray sources seen in scattered light are analogous to “light echos” seen around some supernovae (e.g. SN 1987A, Xu, Croots & Kunkel 1995).

Scattered X-rays observed at an angle θ from the line-of-sight to a GRB arrive after the direct emission with a time-delay τ_s given by:

Electronic address: sav2@star.le.ac.uk

¹ Department of Physics & Astronomy, University of Leicester, Leicester LE1 7RH, United Kingdom.

² Laboratory for High Energy Astrophysics, Code 662, NASA Goddard Space Flight Center, Greenbelt Road, Greenbelt, MD 20771, USA.

³ Universities Space Research Association

⁴ Niels Bohr Institute for Astronomy, Physics and Geophysics, University of Copenhagen, Julian-Maries Vej 30, DK-2100, Copenhagen Ø, Denmark.

⁵ XMM-Newton SOC, Villafranca, Apartado 50727, E-28080 Madrid, Spain.

$$\tau_s = \frac{(1 + z_s) D_s D_g \theta^2}{2c D_{gs}}, \quad (1)$$

where z_s and D_s are the redshift and angular diameter distance of the scattering dust, D_g is the angular diameter distance of the GRB and D_{gs} is the angular diameter distance from the dust to the GRB (Miralda-Escudé 1999).

Here we discuss the case of GRB 031203 observed by *XMM-Newton* on two occasions shortly after the burst. The first observation revealed the first dust-scattered X-ray halo detected around a GRB.

2. OBSERVATIONS AND DATA ANALYSIS

GRB 031203 was detected by the IBIS instrument on *Integral* on 2003 December 3 at 22:01:28 UT as a single peaked burst with a duration of 30 s and peak flux of 1.3×10^{-7} erg s⁻¹ cm⁻² in the 20–200 keV band (Gotz et al. 2003; Mereghetti & Gotz 2003). A 58 ks *XMM-Newton* observation of the field began at 2003 December 4, 04:09:29 UT. Several X-ray sources were detected within the 2.5' radius *Integral* error-circle (Santos-Lleó & Calderón 2003), the brightest of which (S1) appeared to fade through the observation (Rodríguez-Pascual et al. 2003) and was interpreted as the X-ray afterglow of GRB 031203. We refined the astrometric position of the afterglow by performing a cross-correlation with the USNO-A2 catalog, the improved S1 position was (J2000) RA=08^h02^m30.19^s, Dec=−39° 51' 04.0" (1 σ error 0.7", Tedds et al. 2003).

The position in the Galactic plane ($l = 255^\circ, b = -4.6^\circ$) results in high optical extinction ($E(B-V) = 1.0$, Schlegel, Finkbeiner & Davis 1998). Optical/IR observations failed to locate an afterglow. Radio observations did locate a transient source location consistent with the X-ray afterglow (Soderberg, Kulkarni & Frail 2003), and optical imaging and spectroscopy revealed a candidate host galaxy at $z = 0.105$ which shows star-forming features typical of GRB hosts (Prochaska et al. 2003a,b). Our refined location for the X-ray afterglow is within 0.5" of the optical galaxy and consistent with the position of the radio source.

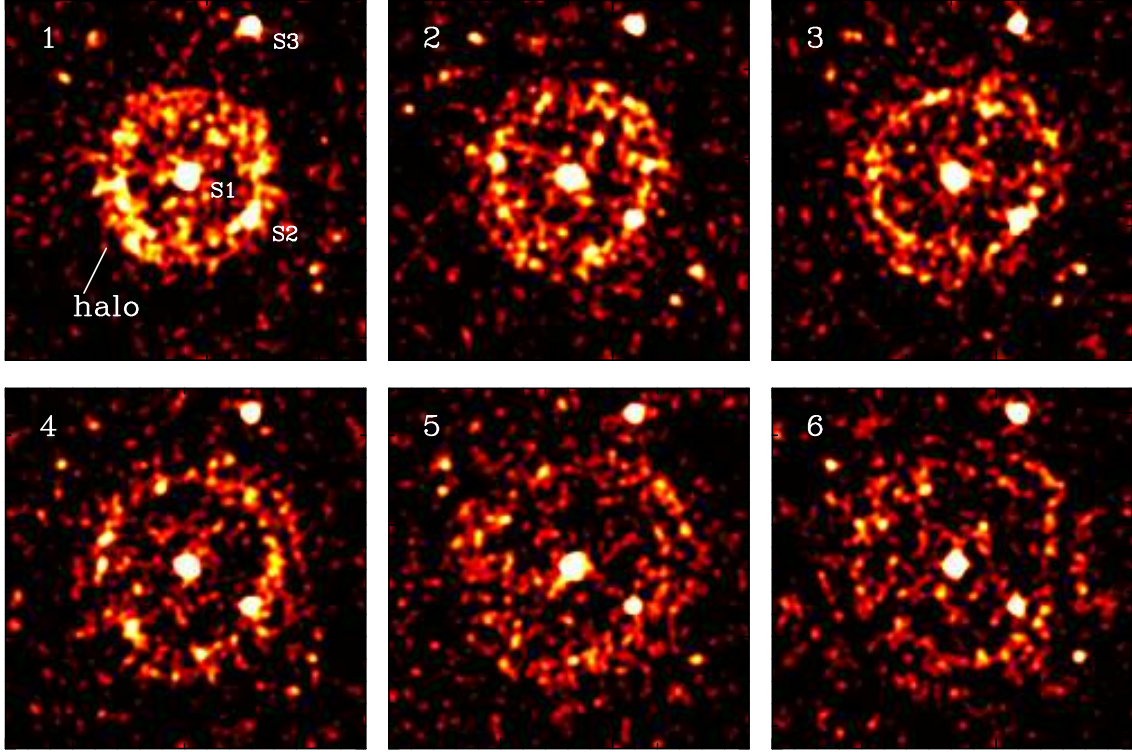


FIG. 1.— Combined MOS images of GRB 031203 covering the $0.7 - 2.5$ keV range, spanning $10'$ on a side. The data were divided into 10 contiguous time intervals lasting 5780 s. The images were obtained from the first six time slices are shown (smoothed using a 6 arcsec Gaussian kernel). The three brightest point sources (S1, S2, S3) are marked.

During the first *XMM-Newton* observation the GRB was observed on axis with all EPIC instruments in full-frame modes (Strüder et al. 2001; Turner et al. 2001). A second 54 ks *XMM-Newton* observation was obtained on 2003 December 6 in which the GRB was $\approx 6'$ off axis. The observational details and the GRB spectrum and light-curve are discussed in detail in Watson et al. (2004).

The extraction of science products followed standard procedures using the *XMM-Newton* Science Analysis System (SAS v5.4.1). The EPIC data were processed using the SAS chains to produce calibrated event lists and remove background flares. GRB afterglow source counts were extracted from circular regions (radius $34''$) and background counts were estimated from a large off-axis region free from obvious point sources and the halo. The GRB afterglow fades as $(t - t_0)^{-0.4}$, where t_0 is the time of the GRB, which is unusually slow for GRB X-ray afterglows.

3. THE X-RAY HALO

The X-ray image from the first *XMM-Newton* observation reveals an extended, circular halo concentric with the GRB 031203 afterglow (see Fig. 1). This halo was seen in all three cameras of the EPIC instrument, is unique to this observation, and is not due to scattered optical or X-ray light within the instrument. Summing the entire observation the halo had the form of a virtually complete ring (Vaughan et al. 2003), but splitting the observation into contiguous time intervals revealed distinct rings which increased in radius through the observation.

In order to better quantify this expansion, EPIC MOS images were produced for ten contiguous time intervals

of 5780 s duration, spanning the entire first observation, and binned to $4''$ pixels. We concentrate on the MOS data as the halo lies over several chip gaps in the EPIC pn images, but the same halo was seen in both. The radial profiles of the images about the afterglow were calculated removing the three brightest point sources within the region of interest (S1, S2 and S3 in Fig. 1) by ignoring all counts within $40''$ from the centroid of each source. The radial profiles were then background subtracted using the mean level from the $350 - 400''$ annulus, which is well outside the detected halo. The resulting count profiles as a function of radius are shown in Fig. 2. The strongest peak moved outward from $\sim 120''$ to $\sim 220''$ during the observation, while a second peak moved from ~ 160 to $\sim 270''$.

The radial positions of the two rings were measured from the local maxima of the two peaks in the radial distributions. Fig. 3 shows the change in radii as a function of time, and both were well fit by a simple power-law ($\theta \propto (t - t_0)^\alpha$). Fixing $t_0 = 0$, the indices of the power-law expansions were measured to be $\alpha = 0.53 \pm 0.04$ and 0.51 ± 0.05 for the inner and outer rings respectively (errors are 90% confidence intervals), consistent with the $\theta \propto (t - t_0)^{1/2}$ expansion predicted for a scattered halo. As a consistency check we allowed t_0 to be a free parameter but fixed $\alpha = 0.5$ and refitted to derive limits of $t_0 = 2794^{+2765}_{-3178}$ s and 2005^{+2512}_{-2867} s for the inner and outer ring respectively, both consistent with $t_0 = 0$. The second *XMM-Newton* observation obtained 3 days after the burst showed no evidence for any ringed structure.

The distance to the GRB is large (adopting the redshift of the putative host galaxy), the time-delay is short

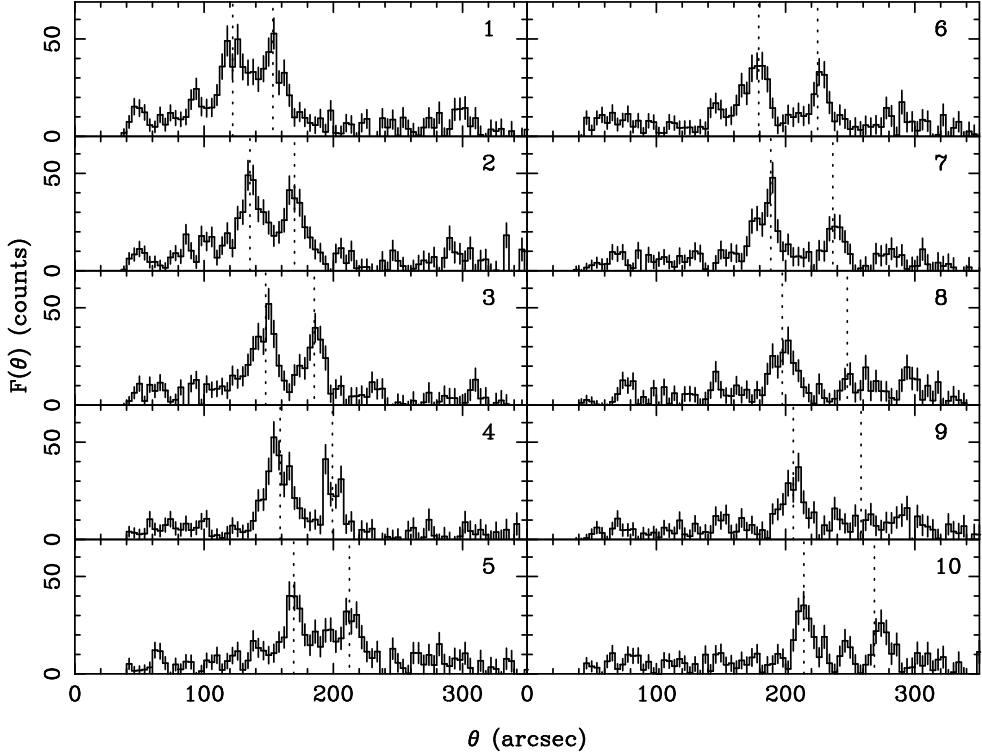


FIG. 2.— Radial profile of counts about the GRB 031203 afterglow from ten contiguous time intervals (derived from the combined MOS 0.7–2.5 keV images). The afterglow itself (S1) and the next two brightest point sources (S2, S3) are removed prior to calculating the profiles (the positions of S2 and S3 are marked in the upper panels). The two peaks corresponding to the two expanding rings are obvious. The dotted lines denote the best-fitting $\theta \propto (t - t_0)^{1/2}$ functions (see Fig. 3).

and θ is relatively large, thus to a good approximation $D_g = D_{gs}$ and $(1 + z_s) = 1$ in equation (1), hence $D_s = 2c\tau_s/\theta^2$. Assuming $\theta \propto (t - t_0)^{1/2}$ and $t_0 = 0$, the data in Fig. 3 imply that the scattering dust slabs are located at distances from the observer of $D_1 = 1388 \pm 32$ pc and $D_2 = 882 \pm 20$ pc, corresponding to the inner and outer ring respectively. At these distances, the ring diameters probe size scales of 2–3 pc in the dust scattering medium.

The halo spectrum was extracted from an annulus with radii $110 - 220''$ using only the first half of the observation; the decreased surface brightness of the halo at later times makes spectral extraction unreliable. A background spectrum was extracted from a large off-axis region (avoiding the halo and other point sources). Fig. 4 shows the halo spectrum compared to the afterglow spectrum. The spectrum of the halo is much steeper than that of the afterglow. Fitting with a simple absorbed power-law yielded photon indices of $\Gamma = 1.98 \pm 0.05$ and $\Gamma = 3.03 \pm 0.14$ for the afterglow and halo, respectively. The best-fitting absorbing column was $N_{\text{H}} = 8.8 \pm 0.5 \times 10^{21} \text{ cm}^{-2}$ when fixed to be the same for both afterglow and halo spectra. This is larger than the Galactic value of $N_{\text{H}} = 6.1 \times 10^{21} \text{ cm}^{-2}$ (Dickey & Lockman 1990). The specific fluxes at $t = 36650$ s after the burst at 1 keV are $1.5_{-0.1}^{+0.2} \times 10^{-4}$ photons $\text{cm}^{-2} \text{ s}^{-1} \text{ keV}^{-1}$ for the afterglow and $6.0 \pm 0.4 \times 10^{-4}$ photons $\text{cm}^{-2} \text{ s}^{-1} \text{ keV}^{-1}$ for the halo.

To model the dust scattering medium, we have simultaneously fitted the ten radial profiles shown in Fig. 2 using the differential and total scattering cross sections of

the Rayleigh-Gans approximation (Mauche and Gorenstein 1986). This is a valid approximation if the grain radius in μm is much less than the X-ray photon energy in keV (Smith & Dwek 1998). We assume that the dust is confined to two slabs at distances D_1 and D_2 with thickness ΔD . The halo seen is created by the combination of the soft X-ray pulse from the GRB and the subsequent afterglow. The observed angular width of the rings results from a combination of the duration of the soft X-ray pulse, Δt , ΔD and the point spread function (PSF) of the telescope. The width of the PSF corresponds to $\Delta t \sim 1000$ s or $\Delta D \sim 100$ pc. Given that the GRB is very short, ~ 30 s (Mereghetti & Gotz 2003), we assume that $\Delta t \ll 1000$ s and hence, allowing for the PSF, the observed broadening of the rings, $20''$, gives us an estimate of the slab thickness, $\Delta D = 130 \pm 50$ pc.

The angular and temporal distribution was well fitted using grains with radii in the range $0.15 < a < 0.25 \mu\text{m}$. Smaller grains scatter to much larger angles (not visible because the time elapsed since the burst is too small) and the upper limit to the grain size distribution is expected to be $\approx 0.3 \mu\text{m}$ (Predehl et al. 1991). Using this range of grain sizes, we require the initial GRB pulse and afterglow to have a photon index of $\Gamma \sim 2.0$ (as observed for the afterglow from 6 h) to match the observed photon index of the halo ($\Gamma = 3.0$).

The brightness of the halo depends on the product of the differential scattering cross sections of the grains, the column densities of the grains in the slabs and the integrated flux of the X-ray pulse and afterglow. Interstellar extinction maps show structure in the GRB direction, with a considerable increase to $A_V \approx 2$ mag at a dis-

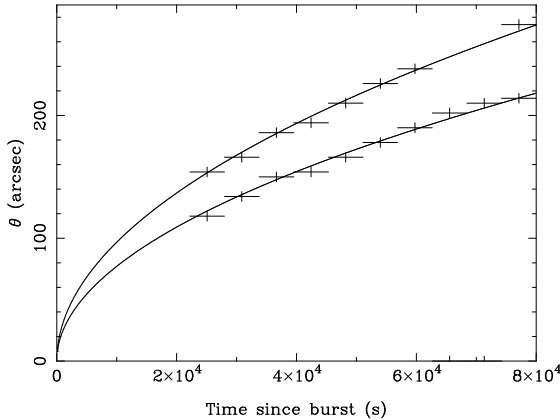


FIG. 3.— Expansion of the two rings around GRB 031203 with time. The radius of each ring was measured from the local maxima of the radial profiles (Fig. 2). In both cases the expansion was well-fitted with a functional form $\theta \propto (t - t_0)^{1/2}$. The errors were assumed to be the width of the bin size used for the radial profile measurement.

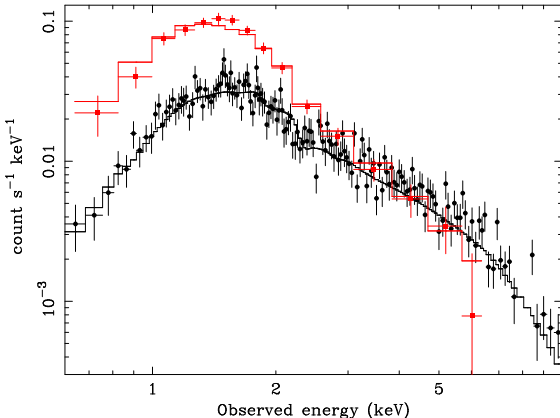


FIG. 4.— Absorbed power-law model fits to the EPIC pn spectra of the GRB 031203 afterglow (circles, thick line) integrated over the entire observation and the dust halo (squares, thin line) integrated over the first half (27895 s) of the observation (during which the surface brightness was high enough for a reasonable spectral extraction). This clearly demonstrates the spectrum of the halo is significantly steeper than the afterglow.

tance of ~ 1.3 kpc (Neckel & Klare 1980). This distance is consistent with the location of the more distant dust slab we detect. Adopting a mean grain size of $a = 0.2$ μm , an $A_V = 2$ mag corresponds to a grain column density of $1.5 \times 10^8 \text{ cm}^{-2}$ (Mauche and Gorenstein 1986). The best fit to the ring structure ($\chi^2/\text{d.o.f.} = 836/489$) results from dividing this column density between the two slabs, $N_1 \sim 1 \times 10^8$ and $N_2 \sim 0.5 \times 10^8 \text{ cm}^{-2}$ (i.e. most of the dust is in the more distant slab). Using these values and $a = 0.20 \pm 0.05$, the time-integrated flux required for the soft X-ray pulse is $1600 \pm 800 \text{ photon cm}^{-2} \text{ keV}^{-1}$ at 1 keV. Assuming a 30 s rectangular pulse this is equivalent to ~ 5 Crabs; using $\Gamma = 2$ the predicted GRB flux in the $20 - 200$ keV band is $2.4 \pm 1.2 \text{ photon cm}^{-2} \text{ s}^{-1}$. Given the assumptions (e.g. spectral shape) this is in reasonable agreement with the value reported for GRB 031203 (peak of $\sim 1.2 \text{ photon cm}^{-2} \text{ s}^{-1}$, Gotz et al. 2003; Mereghetti & Gotz 2003). The X-ray burst is very bright compared to the afterglow (see Watson et al. 2004). Extrapolating the decay of the afterglow (section 2) to the time of the GRB accounts for only ~ 2 per cent of the halo emission.

The line of sight to GRB 031203 passes close to the center of the Gum Nebula which appears as a 28° diameter sphere in $\text{H}\alpha$ centered at $l = 258^\circ, b = -2^\circ$ (Chanot & Sivan 1983). The Gum Nebula is likely to be a supershell created by repeated SNe explosions within it. Reynoso & Dubner (1997) detected a neutral gas disk (H I) associated with the Gum Nebula, located $\sim 500 \pm 100$ pc from us, with a radius of ~ 150 pc. The dust slab nearest to us may be associated with the rear face of the Gum Nebula which is known to have a concentration of molecular clouds (Woermann, Gaylard & Otrupcek 2001).

This paper is based on observations obtained with XMM-Newton, an ESA science mission with instruments and contributions directly funded by ESA Member States and the USA (NASA). SV and AJL acknowledge support from PPARC, UK. We acknowledge the benefits of collaboration within the Research and Training Network “Gamma-Ray Bursts: An Enigma and a Tool”, funded by the European Union under contract HPRN-CT-2002-00294. We thank an anonymous referee for a constructive report.

REFERENCES

Chanot, A., Sivan, J.P., 1983, A&A, 121, 19
 Dickey, J.M., Lockman, F.J. 1990, ARA&A, 28, 215
 Draine, B.T. 2003, ApJ, 598, 1026
 Gotz, D., Mereghetti, S., Beck, M., Borkowski, J., Mowlavi, N. 2003, GRB Coordinates Network, 2459
 Klose, S. 1994, A&A, 289, L1
 Mauche, C.W., Gorenstein, P. 1986, ApJ, 302, 371
 Mereghetti, S., Gotz, D. 2003, GRB Coordinates Network, 2460
 Miralda-Escudé 1999, ApJ, 512, 21
 Neckel, Th., Klare, G., A&A Suppl., 42, 251
 Overbeck, J.W. 1965, ApJ, 141, 864
 Prochaska, J., Chen, H.W., Hurley, K., Bloom, J.S., Graham, J.R., Vacca, W.D. 2003, GRB Coordinates Network, 2475
 Prochaska, J., Bloom, J.S., Chen, H.W., Hurley, K., Dressler, A., Osip, D. 2003, GRB Coordinates Network, 2482
 Predehl, P., Bräuniger, Burkert, W., Schmitt, J.H.M.M. 1991, A&A, 246, L40
 Reynoso, E. M., Dubner, G. M. 1997, A&A Suppl., 123, 31
 Rodríguez-Pascual, P., Santos-Lleó, M., Gonzales-Riestra, R., Schartel, N., Altieri, B. 2003, GRB Coordinates Network, 2474
 Rolf, D.P. 1983, Nature, 302, 46
 Santos-Lleó, M., Calderon, P. 2003, GRB Coordinates Network, 2464
 Schlegel, D. J., Finkbeiner, D. P., Davis, M. 1998, ApJ, 500, 525
 Smith, R.K., Dwek, E. 1998, ApJ, 503, 831
 Soderberg, A.M., Kulkarni, S.R., Frail, D.A. 2003, GRB Coordinates Network, 2483
 Strüder, L., et al. 2001, A&A, 365, L18
 Tedds, J., et al. 2003, GRB Coordinates Network, 2490
 Trümper, J., Schönfelder, V. 1973, A&A, 25 445
 Turner, M.J.L., et al. 2001, A&A, 365, L27
 Vaughan, S. et al. 2003, GRB Coordinates Network, 2489
 Watson, D. et al. 2004, ApJ, in preparation
 Woermann, B., Gaylard, M.J., Otrupcek, R. 2001, MNRAS, 325, 1213
 Xu, J., Crotts, A.P.S., Kunkel, W.E. 1995, ApJ, 451, 806